PHYSICAL REVIEW C VOLUME 8, NUMBER 2 AUGUST 1973

Single-Charge Exchange (π^+, π^0) in Light Nuclei

Il-Tong Cheon*
Institut de Physique, Université de Liège, Sart-Tilman, B-4000 Liège 1, Belgium
(Received 15 September 1972; revised manuscript received 26 February 1973)

The total and differential cross sections were calculated for $^{13}C(\pi^+, \pi^0)^{13}N$, considering the effects of double and triple scatterings as well as pion absorption. An attempt is also made to explain the extremely small total cross section for $^{14}N(\pi^+, \pi^0)^{14}O$ compared with other cases ^{10}B, ^{11}B, ^{13}C, and ^{18}O.

1. INTRODUCTION

Recently, a difficulty was reported in the experiments of single-charge-exchange reaction (π^+, π^0) on light nuclei at 180 MeV (lab).[1] As seen in Table I, the total cross sections are in the range of 1 ~ 6 mb except for $^{14}N(\pi^+, \pi^0)^{14}O$ in which the total cross section is about 100 times smaller than the other cases. This fact must be due to nuclear structure and the reaction mechanism. Two attempts were made to find a solution to this problem.

Wilkinson[2] explained it in the following way: "When the reaction involves mirror states, for example, $^{13}C(\pi^+, \pi^0)^{13}N$, the large cross section is expected since the nuclear wave functions do not change. The cases where the analogue state is not involved have significantly small cross sections, in particular $^{14}N(\pi^+, \pi^0)^{14}O$; this presumably reflects the small overlap of the nuclear wave functions that results in the large ft-value for beta-decay." This *qualitative* interpretation may be reasonable as he claimed. However, it is still not clear why the magnitude of total cross section for $^{14}N(\pi^+, \pi^0)^{14}O$ at 180 MeV (lab) should be ~0.05 mb while it is in the range of 1 ~ 6 mb for other targets.

Sakamoto[3] also tried to explain in the impulse approximation the experimental results, in particular for the case of the ^{14}N target, on the basis of the Chew-Low amplitude for pion-nucleon scattering. His opinion is the following: "For the elastic charge-exchange scattering on mirror states, the spin-flip as well as spin-nonflip amplitudes of pion-nucleon scattering contribute to the cross section. When the reaction proceeds dominantly through the spin-flip amplitudes of pion-nucleon scattering, the small cross section is expected because of the poor overlap of the nuclear wave functions. For example, if the reaction is concerned with the states from $J^\pi = 1^+$ to 0^+, the cross section calculated is about 0.1 mb at 180 MeV (lab) for light nuclei even if the radial wave function does not change." Although this opinion is also partly reasonable, it is not complete because according to this logic the small cross section will also be expected for the case of $^{18}O(\pi^+, \pi^0)$-^{18}F in which the transition $0^+ \to 1^+$ occurs; however, the experiment actually showed the large cross section for this case.

The reaction $^{13}C(\pi^+, \pi^0)^{13}N$ was also analyzed by Bjørnenak, Finjord, and Osland[4] on the basis of the Glauber theory. However, it seems adventurous to apply the Glauber theory to the reaction problems in the (33) resonance region. No attempt was made by them to explain the small cross section of $^{14}N(\pi^+, \pi^0)^{14}O$.

In this situation it is worthwhile to give a clear interpretation of the present difficulty.

2. THEORY

This section is devoted to the discussions on (a) an effective interaction in the processes of single-charge-exchange reaction (π^+, π^0); (b) total cross section for the reaction $^{13}C(\pi^+, \pi^0)^{13}N$ when only single scattering is taken into account and when effects of multiple scatterings are considered.

A. Effective Interaction

Although a pion interacts with a nucleon pair in some cases,[5] the single-particle interaction seems to be *favorable* in single-charge-exchange processes. According to a theory of the p-wave interactions of pions with a static nucleon, the scattering matrix is given in the one-pion approximation in terms of the usual pion-nucleon scattering amplitudes.[6]

$$
\begin{aligned}
t &= \frac{v_q}{v_k}\frac{4\pi c^2}{\sqrt{4\omega_q\omega_k}}\tau_+[3\vec{k}\cdot\vec{q} - (\vec{\sigma}\cdot\vec{k})(\vec{\sigma}\cdot\vec{q})]f_{33}\,,\\
\omega_q &= (c^2\hbar^2\vec{q}^{\,2} + \mu^2c^4)^{1/2}\,, \quad \tau_+ = -\tfrac{1}{2}(\tau_x + i\tau_y)\,,\\
v_q &= d\omega_q/d(\hbar q)\,, \quad \tau_+\begin{pmatrix}p\\ n\end{pmatrix} = \begin{pmatrix}0\\ p\end{pmatrix}\\
f_{33} &= e^{i\delta}\sin\delta/k^3\,,
\end{aligned}
\tag{1}
$$

where $\hbar\vec{q}$ and $\hbar\vec{k}$ denote the momenta of incoming and outgoing pions, respectively, and $\vec{\sigma}$ and $\vec{\tau}$ are spin and isospin operators. Because the (33) reso-

TABLE I. Cross sections of single-charge-exchange reaction (π^+, π^0) at 180 MeV.

Reaction	Total cross section (mb)
$^{10}B(\pi^+, \pi^0)^{10}C$	1.3 ± 0.2
$^{11}B(\pi^+, \pi^0)^{11}C$	6.4 ± 1.1
$^{13}C(\pi^+, \pi^0)^{13}N$	4.1 ± 1.3
$^{14}N(\pi^+, \pi^0)^{14}O$	$\lesssim 0.05$
$^{18}O(\pi^+, \pi^0)^{18}F$	4.4 ± 0.9

nance amplitude is dominant in the energy region considered here, we neglected other terms. Although the recoil of the nucleon is usually neglected in the static model, it is considered here even though it is small in magnitude. When the recoil momentum of the nucleon is described by $\vec{S}$ (which is equal to $\hbar\vec{q} - \hbar\vec{k}$ by momentum conservation) we obtain, considering $\vec{S} = -i\hbar\vec{\nabla}$, the effective interaction

$$t_j = \frac{v_q}{v_k} \frac{4\pi\hbar^2 c^2}{(4\omega_q \omega_k)^{1/2}} (2\pi)^3 \delta(\vec{r}_0 - \vec{r}_j)\tau_+ \times \{2\vec{q}^2 + 2i\vec{q}\cdot\vec{\nabla}_j - \vec{\sigma}_j \cdot [\vec{q}\times\vec{\nabla}_j]\} f_{33}, \qquad (2)$$

where j denotes the jth nucleon in the nucleus. In the derivation of Eq. (2) from (1) we used the relation

$$(\vec{\sigma}\cdot\vec{A})(\vec{\sigma}\cdot\vec{B}) = \vec{A}\cdot\vec{B} + i\vec{\sigma}\cdot(\vec{A}\times\vec{B}). \qquad (3)$$

The second term in Eq. (2) is independent of spin. This term can also cause transitions with $\Delta J = 1$. This situation is very different from the discussion given in Ref. 3 in which it was explained that only the spin-flip term can cause such a transition as $1^+ \rightleftarrows 0^+$. Actually, the first term in Eq. (2) is the dominant contribution to the matrix elements, in which the contributions from second and third terms are smaller by about two orders of magnitude. This will be seen later in the numerical discussion.

B. Total Cross Section for $^{13}C(\pi^+,\pi^0)^{13}N$

In our present model the target nucleus is constructed by a core nucleus and the nucleon by which a pion is scattered. We choose a simple harmonic-oscillator wave function for the scatterer.

$$\Phi_f([(1)_n]^{p_{1/2}}; [(2345)_n(6789)_p]^{p_{3/2}}; [(10\,11)_n(12\,13)_p]^{s_{1/2}}) \quad \text{for the } ^{13}\text{C nucleus}.$$

When the pion is scattered by the $p_{1/2}$ neutron in the ^{13}C nucleus, the ground-state wave function is given as

$$\Psi^{1/2-1/2}_{1/2\,M}(^{13}\text{C}) = NA \sum_{\lambda\nu\kappa} \langle \lambda\nu \tfrac{1}{2}\kappa \,|\, \tfrac{1}{2}M\rangle \sum_T \langle T0\tfrac{1}{2} - \tfrac{1}{2} \,|\, \tfrac{1}{2} - \tfrac{1}{2}\rangle \phi^{1/2-1/2}_{1/2\kappa}(1)\Phi^{T0}_{\lambda\nu}(23\cdots 13),$$
$$\phi^{1/2-1/2}_{1/2\kappa}(1) = \sum_{m\mu} \langle 1m\tfrac{1}{2}\mu \,|\, \tfrac{1}{2}\kappa\rangle Y_{1m}(\hat{r}_1) X_{1/2\mu}\, \chi_{1/2-1/2}\, r_1 \exp(-\tfrac{1}{2}\beta r_1^2), \qquad (4)$$

where subscripts denote the total spins and their components, the superscripts denote the total isospins, and $X_{1/2\mu}$ and $\chi_{1/2-1/2}$ are the spin and isospin states, respectively. N is the normalization constant and A is the antisymmetrization operator. The wave function of the residual nucleus ^{13}N is also constructed in the same manner.

1. Single-Scattering Cross Section

The matrix element describing a single scattering of a pion is obtained by calculating the quantity $\langle \Psi_f | t | \Psi_i \rangle$ with the effective t matrix given in Eq. (2). The general form of matrix element is given as

$$\mathfrak{M} = N^2 \frac{\sqrt{\pi}}{\beta^{5/2}} e^{-\xi} e^{\xi\cos\theta} q^2 [(\delta_{++} + \delta_{--})\{A_1 + A_2 b_1^2 + A_3 b_1^4\} + (\delta_{+-} - \delta_{-+})\sin\theta\{A_4 + A_5 b_1^2\}],$$
$$\xi \equiv q^2/2\beta, \quad b_1 = \sin(\theta/2), \qquad (5)$$

where A_i's are the functions of β and q^2, θ is the scattering angle, and δ_{++} etc. are the symbols of the total spin quantum number (JM) in the final and initial states of the nuclei, namely, δ_{+-} denotes $(J' = \frac{1}{2},\ M' = \frac{1}{2})$ for ^{13}N and $(J = \frac{1}{2},\ M = -\frac{1}{2})$ for ^{13}C. Then, we have the differential and total cross sections

$$\frac{d\sigma(\pi^+, \pi^0)}{d\Omega} = F \frac{1}{2J+1} \sum_{MM'} |\mathfrak{M}|^2, \qquad (6)$$

$$\sigma(\pi^+, \pi^0) = FD(\beta, q^2), \qquad (7)$$

where

$$F = \frac{2\pi\hbar k^2}{v_q v_k} \left(\frac{1}{2\pi\hbar}\right)^3 \left(\frac{\hbar^2 c^2}{(4\omega_q\omega_k)^{1/2}}\right)^2 \left(\frac{4\pi v_q}{v_k}\right)^2 |f_{33}|^2, \qquad (8)$$

$$\frac{1}{2J+1}\sum_{MM'}|\mathfrak{M}|^2=N^4\frac{\pi}{\beta^5}e^{-2\xi}e^{2\xi\cos\theta}q^4(B_0-B_1\cos\theta+B_2\cos^2\theta-B_3\cos^3\theta+B_4\cos^4\theta) \quad (9)$$

$$D(\beta,q^2)=N^4\frac{4\pi^2}{\beta^2}e^{-2\xi}q^2\left\{\left[B_0+B_2+B_4+\frac{1}{2\xi}(B_1+3B_3)+\frac{1}{4\xi^2}(2B_2+12B_4)+\frac{6}{8\xi^3}B_3+\frac{24}{16\xi^4}B_4\right]\sinh(2\xi)\right.$$
$$\left.-\left[B_1+B_3+\frac{1}{2\xi}(2B_2+4B_4)+\frac{6}{4\xi^2}B_3+\frac{24}{8\xi^3}B_4\right]\cosh(2\xi)\right\}, \quad (10)$$

$$B_0=(A_1+\tfrac{1}{2}A_2+\tfrac{1}{4}A_3)^2+(A_4+\tfrac{1}{2}A_5)^2,$$
$$B_1=(A_1+\tfrac{1}{2}A_2+\tfrac{1}{4}A_3)(A_2+A_3)+A_5(A_4+\tfrac{1}{2}A_5),$$
$$B_2=\tfrac{1}{2}A_3(A_1+\tfrac{1}{2}A_2+\tfrac{1}{4}A_3)+\tfrac{1}{4}(A_2+A_3)^2-A_4(A_4+A_5),$$
$$B_3=\tfrac{1}{4}A_3(A_2+A_3)-A_5(A_4+\tfrac{1}{2}A_5),$$
$$B_4=\tfrac{1}{16}A_3{}^2-\tfrac{1}{4}A_5{}^2.$$

Here, the same harmonic-oscillator parameter is chosen for ^{13}N and ^{13}C. The A_i's are given in Table II. The meanings of the notations are the following:
(i) when the antisymmetrization is neglected: $\mathfrak{M}_{11}$ is the contribution from the term q^2 in the effective t matrix (2); $\mathfrak{M}_{12}$ is the contribution from the term $\vec{q}\cdot\vec{\nabla}$ in the effective t matrix (2); $\mathfrak{M}_{13}$ is the contribution from the term $\vec{\sigma}\cdot[\vec{q}\times\vec{\nabla}]$ in the effective t matrix (2); $\mathfrak{M}_{14}=(\mathfrak{M}_{11}+\mathfrak{M}_{12}-\mathfrak{M}_{13})$, the total contribution;
(ii) when the antisymmetrization is taken into account: the $\mathfrak{M}_{1j}$'s are replaced by the $\mathfrak{M}_{2j}$.

In order to compare the contributions from the matrix elements given above, the numerical values of $1/(2J+1)\sum_{MM'}(\mathfrak{M}_{ij})^2$ for each case are tabulated in Table III. In these calculations we used the parametrized phase shift[7]

$$f_{33}=(4.108+0.7987k^2-0.8337k^4-ik^3)^{-1}.$$

It is easily seen in Table III that the essential contributions to the total cross section come from the first term of the effective interaction, namely, the q^2 term. For example, at 180 MeV, the contributions from the term $\vec{q}\cdot\vec{\nabla}$ and $\vec{\sigma}\cdot(\vec{q}\times\vec{\nabla})$ are smaller by two orders of magnitude than the contribution from the term q^2. This tendency remains even if multiple scatterings are taken into account. This fact is very important for understanding why the total cross section of the reaction ^{14}N$(\pi^+,\pi^0)^{14}$O at 180 MeV is 100 times smaller than the other cases. The detailed discussions will be given in the last section.

2. *Effects of Double and Triple Scatterings*

The recent investigations of high-energy hadron scattering have proved the importance of the effects of double scattering. In order to estimate these effects, we use the multiple-scattering formulas given by Watson.[8]

The ground-state expectation value of the multiple-scattering matrix for the elastic scattering can be written as

$$\langle t\rangle=\sum_j\langle t_j\rangle+\sum_j\langle t_j\rangle\,1/(E_0-h_\pi+i\epsilon)\langle t\rangle, \quad (11)$$

where E_0 is the energy of the penetrating pion and h_π is its free Hamiltonian. Here j stands for the

TABLE II. Matrix elements for various cases. The meanings of $\mathfrak{M}$'s are given in the text.

	A_1	A_2	A_3	A_4	A_5
$\mathfrak{M}_{11}$	1	$-\frac{2q^2}{3\beta}$			
$\mathfrak{M}_{12}$		1	$-\frac{2q^2}{3\beta}$	$\frac{1}{9}$	
$\mathfrak{M}_{13}$		$\frac{2}{3}$		$\frac{1}{36}$	$-\frac{q^2}{18\beta}$
$\mathfrak{M}_{14}$	1	$\frac{1}{3}-\frac{2q^2}{3\beta}$	$-\frac{2q^2}{3\beta}$	$\frac{1}{12}$	$\frac{q^2}{18\beta}$
$\mathfrak{M}_{21}$	17	$-\frac{34q^2}{3\beta}$			
$\mathfrak{M}_{22}$		25	$-\frac{50q^2}{3\beta}$	$\frac{1}{9}(13-4\sqrt{2})$	
$\mathfrak{M}_{23}$		$-\frac{14}{3}$		$-\frac{1}{36}(15+16\sqrt{2})$	$\frac{(27+20\sqrt{2})q^2}{90\beta}$
$\mathfrak{M}_{24}$	17	$\frac{89}{3}-\frac{34q^2}{3\beta}$	$-\frac{50q^2}{3\beta}$	$\frac{67}{36}$	$-\frac{(27+20\sqrt{2})q^2}{90\beta}$

jth nucleon in the nucleus and t_j is given in Eq. (2) except for inclusion of the operators, τ_0 and τ_-. It follows that the pion obeys the Schrödinger equation

$$(E_0 - h_\pi - \sum_j \langle t_j \rangle)\phi_\pi = 0 \qquad (12)$$

inside the nucleus. When we assume that the recoil momentum of the nucleon is small, we have

$$\langle \vec{x}' | t_c | \vec{x} \rangle \simeq \frac{A}{V}(2\pi\hbar)^3 \delta(\vec{x}' - \vec{x}) \langle \vec{p} | t_j | \vec{p} \rangle \rho(\vec{x}), \qquad (13)$$

where $t_c = \sum_j \langle t_j \rangle$, $\langle \vec{p} | t_j | \vec{p} \rangle$ denotes an average of the scattering matrix t_j over the spins and isospins of the nucleons in the nucleus, $\rho(\vec{x})$ is the nucleon density, and V and A are the nuclear volume and the mass number. Thus, the Schrödinger equation which the pion obeys is

$$(E_0 - h_\pi - V_c \rho(\vec{x}))\phi_\pi = 0, \qquad (14)$$

where $V_c = A/V(2\pi\hbar)^3 \langle \vec{p} | t_j | \vec{p} \rangle$ which is the potential felt by the pion inside the nucleus and can be connected to the forward scattering amplitude for pion-nucleon scattering.

The scattering series given by Watson is actually not of much practical use unless one can also make the impulse approximation for each scattering. Therefore, in our present calculation, we also make the impulse approximation for each scattering. Since the incident pion energy is high compared with the nuclear excitation energies and the momentum transfer is small, the nucleon excitation can be neglected and we use the closure approximation for the multiple scattering. Under these approximations, Eq. (11) was actually obtained. Namely, the double-scattering term in Eq. (11) may be written as

$$\sum_{j \neq m} \sum_n \int d^3k \frac{\langle f | t_j | k, n \rangle \langle k, n | t_m | i \rangle}{E_0 - E_n(k) + i\epsilon}, \qquad (15)$$

where E_0 and E_n are the pion energies in the initial and intermediate states. In the present calculation, we took the on-energy-shell assumption which was used by Pendleton[9] in the calculation of the double-scattering contribution for the pion elastic scattering by a deuteron at 142 MeV.

The numerical results are shown in Figs. 1 and 2. The total cross sections calculated by our theory have peaks around 145 MeV, which are shifted to a lower energy as compared with the case of a pion-nucleon scattering. This is due to the momentum of the bound nucleon. Only one experimental point is available.[1] Our results are consistent with those given in Refs. 3 and 4. The tendency that the total cross section increases when

TABLE III. The numerical values of $1/(2J+1)\sum_{MM'} |\mathfrak{M}_{ij}|^2$ with $\beta = 0.25$ fm^{-2}. E_L is the incident energy of pion in the laboratory system.

E_L (MeV) \ (ij)	(11)	(12)	(13)	(14)	(21) $(\times 10^5)$	(22)	(23) $(\times 10^2)$	(24) $(\times 10^5)$
70	7.35×10^2	24.2	41.9	7.97×10^2	2.12	1.05×10^4	23.2	3.09
80	9.03×10^2	26.9	39.7	9.87×10^2	2.61	1.16×10^4	22.3	3.63
90	1.10×10^3	29.9	37.7	1.21×10^3	3.19	1.28×10^4	21.4	4.29
100	1.34×10^3	32.5	36.0	1.46×10^3	3.87	1.38×10^4	20.8	5.05
110	1.61×10^3	34.4	34.5	1.74×10^3	4.64	1.43×10^4	20.2	5.90
120	1.88×10^3	35.3	32.7	2.02×10^3	5.44	1.43×10^4	19.5	6.76
130	2.12×10^3	34.6	30.2	2.25×10^3	6.12	1.36×10^4	18.3	7.44
140	2.22×10^3	31.7	26.4	2.35×10^3	6.43	1.20×10^4	16.3	7.69
150	2.15×10^3	26.9	21.4	2.26×10^3	6.21	0.980×10^4	13.5	7.31
160	1.90×10^3	21.0	16.1	1.99×10^3	5.50	0.738×10^4	10.3	6.39
170	1.57×10^3	15.4	11.4	1.64×10^3	4.55	0.521×10^4	7.44	5.22
180	1.24×10^3	10.9	7.79	1.29×10^3	3.60	0.353×10^4	5.17	4.09
190	9.64×10^2	7.59	5.25	9.96×10^2	2.79	0.237×10^4	3.55	3.13
200	7.42×10^2	5.28	3.54	7.65×10^2	2.14	0.159×10^4	2.43	2.39
210	5.73×10^2	3.73	2.41	5.89×10^2	1.66	0.108×10^4	1.69	1.83
220	4.46×10^2	2.64	1.66	4.58×10^2	1.29	0.736×10^3	1.18	1.42
230	3.51×10^2	1.90	1.17	3.59×10^2	1.01	0.516×10^3	0.842	1.11
240	2.79×10^2	1.40	0.829	2.85×10^2	0.806	0.364×10^3	0.609	0.877
250	2.24×10^2	1.04	0.599	2.29×10^2	0.647	0.265×10^3	0.447	0.701
260	1.82×10^2	0.774	0.438	1.85×10^2	0.525	0.191×10^3	0.332	0.566
270	1.49×10^2	0.589	0.325	1.51×10^2	0.430	0.139×10^3	0.250	0.461
280	1.23×10^2	0.448	0.244	1.25×10^2	0.355	0.105×10^3	0.191	0.379
290	1.02×10^2	0.354	0.185	1.04×10^2	0.295	0.791×10^2	0.147	0.314
300	8.56×10	0.273	0.142	8.68×10	0.247	0.571×10^2	0.114	0.263

the multiple scattering is taken into account is also in accord with the results obtained by Bjornenak, Finjord, and Osland[4] who calculated them using the Glauber theory.

It is worthwhile to notice that there is a sharp dip around 50° and a large peak at 65° in the differential cross sections. The existence of the deep dip at 50° is also reported by Bjornenak, Finjord, and Osland.[4] It can be seen in Fig. 2 that the effects of multiple scattering appear in the forward scattering.

3. DISCUSSIONS

In this section, some discussions are given for the cases of ^{10}B, ^{11}B, ^{14}N, and ^{18}O. Only the total cross section of the single-charge-exchange reaction ^{14}N(π^+, π^0)^{14}O at 180 MeV (lab) is so small compared with other cases, as seen in Table I. It is worthwhile to notice that the measurements were done by the activation method.

First of all, let us construct the ground state of the nuclei as follows: two valence nucleons are coupled to the core nucleus. However, in the cases of ^{11}B, ^{11}C, ^{13}C, and ^{13}N, one p-shell nucleon is coupled to the core nucleus. ^{12}C is taken as a core nucleus for ^{14}N and ^{14}O, and ^{16}O for ^{18}O and ^{18}F, because ^{12}C and ^{16}O are the nuclei in which just $1p_{3/2}$ and $1p_{1/2}$ states are occupied. However, in the cases of ^{10}B and ^{10}C, both ^{8}Be and ^{8}B can be candidates for a core nucleus because in these cases the $1p_{3/2}$ state is not completely occupied by nucleons. It is easy to evaluate the possible states which the valence nucleons can have. For example, let us look at the case of ^{14}N (1^+, $T=0$ g.s.). If the core nucleus ^{12}C is in the ground state (0^+, $T=0$), the two valence nucleons have $T=0$, $S=1$ and $l=0,2$. The state $l=1$ is dropped because it has the wrong parity. Then, the total spins of the valence nucleons are $J^{\pi}{}_{pn}=1^+, 2^+, 3^+$ for $l=2$. Only $J^{\pi}{}_{pn}=1^+$ can couple to the total spin

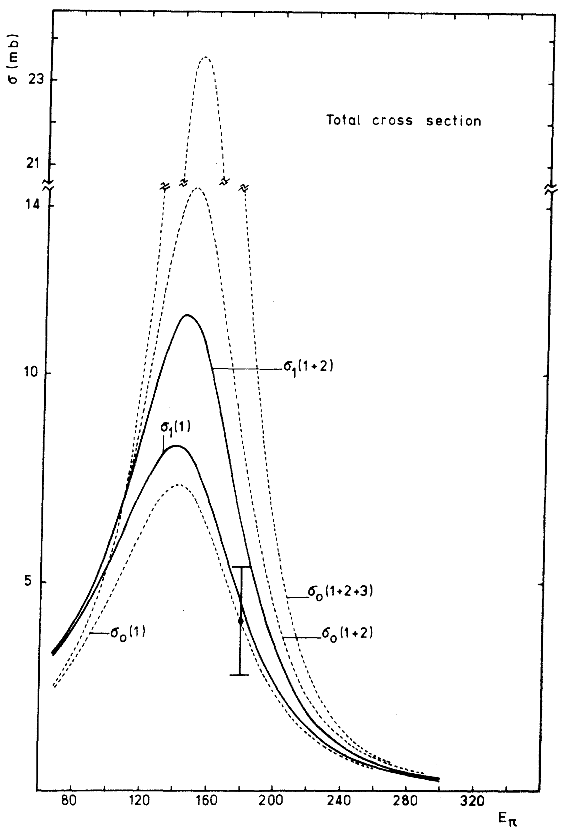

FIG. 1. Total cross section for ^{13}C(π^+, π^0)^{13}N without pion absorption effects. σ_0 and σ_1 correspond to the total cross sections without and with antisymmetrization of the wave functions, respectively. $\sigma(1)$: only single scattering, $\sigma(1+2)$; both the single scattering and the double scattering are taken into account. $\sigma(1+2+3)$: multiple scatterings up to triple scattering are taken into account. Experimental data are taken from Ref. 1.

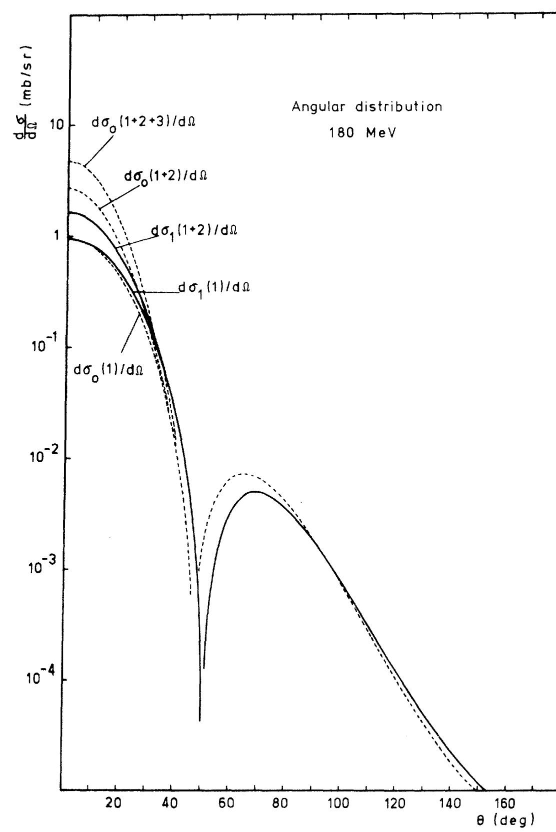

FIG. 2. Angular distributions for ^{13}C(π^+, π^0)^{13}N at 180 MeV (lab). The notations are the same as those given in Fig. 1.

TABLE IV. Ground states of nuclei for the case that only the ground state of the core nucleus is taken into account. The third column denotes the possible states which the valence nucleons can have.

Nucleus	Mode	States of the valence nucleons l	s	T	j^{π}
^{10}B (3^+, $T=0$)	^{8}Be (0^+, $T=0$) + (pn)	2	1	0	3^+
	^{8}B (2^+, $T=1$) + (nn)	2	0	1	2^+
^{10}C (0^+, $T=1$)	^{8}Be (0^+, $T=0$) + (pp)	0	0	1	0^+
	^{8}B (2^+, $T=1$) + (pn)	2	0	1	2^+
		2	1	0	2^+
^{14}N (1^+, $T=0$)	^{12}C (0^+, $T=0$) + (pn)	0	1	0	1^+
		2	1	0	1^+
^{14}O (0^+, $T=1$)	^{12}C (0^+, $T=0$) + (pp)	0	0	1	0^+
^{18}O (0^+, $T=1$)	^{16}O (0^+, $T=0$) + (nn)	0	0	1	0^+
^{18}F (1^+, $T=0$)	^{16}O (0^+, $T=0$) + (pn)	0	1	0	1^+
		2	1	0	1^+

of the core nucleus ^{12}C (0^+, $T=0$) to produce the total spin of the nucleus ^{14}N (1^+, $T=0$). Thus, the possible states of the valence nucleons (pn) are ($l=0$, $s=1$, $T=0$, $J^{\pi}{}_{pn}=1^+$) and ($l=2$, $s=1$, $T=0$; $J^{\pi}{}_{pn}=1^+$). In the similar manner, we can construct the ground state of the nucleus ^{14}N even when the excited states of the core nucleus ^{12}C are taken into account. In Table IV some examples are given when the core nuclei are in the ground states. It is easily seen that the matrix elements

$$\langle F|\tau_{j+}\vec{0}_j(\vec{q}\cdot\vec{\nabla}_j)|I\rangle$$

and/or

$$\langle F|\tau_{j+}\vec{0}_j\vec{\sigma}_j(\vec{q}\times\vec{\nabla}_j)|I\rangle$$

can remain for all cases including ^{11}B(π^+, π^0)^{11}C and ^{13}C(π^+, π^0)^{13}N, where $\vec{0}_j=\exp[i(\vec{k}-\vec{q})\cdot\vec{r}_j]$. The matrix element $\langle F[\tau_{j+}\vec{0}q^2]I\rangle$ makes large contributions to the total cross sections for the isobaric mirror charge-exchange reactions ^{11}B(π^+, π^0)^{11}C and ^{13}C(π^+, π^0)^{13}N since the nuclear wave functions do not change with the operator $(\tau_{j+}\vec{0}_j q^2)$, namely the wave function obtained after τ_{j+} operates on the initial state is the same one as the final state. As we saw already in the previous section (see Table III), at 180 MeV (lab), the contribution of the matrix element $\langle F|\tau_{j+}\vec{0}_j q^2|I\rangle$ to the total cross section is larger by a factor of 10^2 than the contributions from the others, $\langle F|\tau_{j+}\vec{0}_j(\vec{q}\cdot\vec{\nabla}_j)|I\rangle$ and $\langle F|\tau_{j+}\vec{0}_j\vec{\sigma}_j\cdot(\vec{q}\times\vec{\nabla}_j)|I\rangle$. However, in the cases of ^{10}B(π^+, π^0)^{10}C, ^{14}N(π^+, π^0)-^{14}O, and ^{18}O(π^+, π^0)^{18}F, the wave functions obtained after the operator τ_{j+} acts on the initial states are not the same ones as the final-state wave functions. Therefore, contributions of the matrix element $\langle F|\tau_{j+}\vec{0}q^2|I\rangle$ to the total cross section decrease because of the poor overlap of the nuclear wave functions. This is reflected in the comparatively small cross sections as seen in Table I, except the case of ^{18}O(π^+, π^0)^{18}F. Next, let us compare the case of ^{10}B(π^+, π^0)^{10}C with that of ^{14}N(π^+, π^0)-^{14}O. When the operator τ_{j+} acts on the ground states $|^{10}\mathrm{B}(3^+, T=0)\rangle$ and $|^{14}\mathrm{N}(1^+, T=0)\rangle$, we obtain

$$\tau_{j+}|^{10}\mathrm{B}(3^+, T=0)\rangle=\tau_{j+}|(^8\mathrm{Be}+pn) \quad \text{or} \quad (^8\mathrm{B}+nn)\rangle$$

$$=|^{10}\mathrm{C}(3^+, T=1)\rangle$$

and

$$\tau_{j+}|^{14}\mathrm{N}(1^+, T=0)\rangle=\tau_{j+}|(^{12}\mathrm{C}+pn)\rangle=|^{14}\mathrm{O}(1^+, T=1)\rangle$$

The overlaps of the wave functions

$$\langle^{10}\mathrm{C}(0^+, T=1, \mathrm{g.s.})|\vec{0}_j|^{10}\mathrm{C}(3^+, T=1)\rangle$$

and

$$\langle^{14}\mathrm{O}(0^+, T=1, \mathrm{g.s.})|\vec{0}_j|^{14}\mathrm{O}(1^+, T=1)\rangle$$

are actually much smaller than

$$\langle^{11}\mathrm{C}(\tfrac{3}{2}^-, T=\tfrac{1}{2}|\vec{0}_j|^{11}\mathrm{C}(\tfrac{3}{2}^-, T=\tfrac{1}{2})\rangle$$

and

$$\langle^{13}\mathrm{C}(\tfrac{1}{2}^-, T=\tfrac{1}{2})|\vec{0}_j|^{13}\mathrm{C}(\tfrac{1}{2}^-, T=\tfrac{1}{2})\rangle .$$

However, as seen in Table IV, a common state is found among the states of the core nuclei plus the valence nucleons which construct the ground states of ^{10}B and ^{10}C. On the other hand, we cannot find any common state for the cases of ^{14}N and ^{14}O even if eight excited states of the core nucleus ^{12}C (up to 13.35 MeV) are considered. Then, the overlap of the wave functions

$$\langle^{10}\mathrm{C}(0^+, T=1, \mathrm{g.s.})|\vec{0}_j|^{10}\mathrm{C}(3^+, T=1)\rangle$$

seems to be better than that of

$$\langle {}^{14}\text{O}(0^+,\ T=1,\ \text{g.s.})|\vec{0}_j|{}^{14}\text{O}(1^+,\ T=1)\rangle .$$

This results in the larger cross section for ^{10}B-$(\pi^+, \pi^0)^{10}$C than the case of ^{14}N$(\pi^+, \pi^0)^{14}$O.

According to the explanation given above, we should also have a considerably small cross section for ^{18}O$(\pi^+, \pi^0)^{18}$F, but the measured value is very large, 4.4 ± 0.9 mb. This is not surprising because the measurement was done by the activation method which cannot distinguish the low-lying levels from the ground state in the residual nuclei ^{18}F. Since the second excited state of ^{18}F$(0^+, T=1,$ 1.0419 MeV) is indeed included in the measurement, we obtain the large total cross section because

$$\tau_{j^+}|{}^{18}\text{O}(0^+,\ T=0,\ \text{g.s.})\rangle = |{}^{18}\text{F}(0^+,\ T=1)\rangle$$

gives good overlap with the wave function of the second excited state of ^{18}F$(0^+, T=1,$ 1.0419 MeV).

The trivial differences of the total cross sections are due to the Clebsh-Gordan coefficients and nuclear size parameter β (namely, the harmonic-oscillator constant).

It is also interesting to examine the reaction (p, n). The experimental data at 155 MeV are tabulated in Table V.[10] In this case, the total cross section of ^{14}N$(p, n)^{14}$O is also smaller by $\frac{1}{20}$ to $\frac{1}{50}$ than the others. The similar discussion might be given for the reactions (p, n) by considering the form of the interaction

$$V_c(r) + V_{SL}(r)\vec{L}\cdot\vec{S},$$

where r is the distance between the projectile p and the knock-out neutron. Generally, the dominant contribution to the total cross section comes from the central force. The matrix element $\langle F|V_c(r_j)|I\rangle$ is small for ^{14}N$(p, n)^{14}$O and ^{10}B(p, n)-^{10}C, while it is large for ^{11}B$(p, n)^{11}$C and ^{13}C(p, n)-^{13}N. The cross section for the reaction ^{18}O(p, n)-^{18}F will be expected to be very small because the measurement of this reaction can generally distinguish the low-lying levels from the ground state. The small cross section of the reaction ^{14}N(p, n)-^{14}O is considered to be caused by the same reason as for the case of ^{14}N$(\pi^+, \pi^0)^{14}$O. Therefore, both cases should be explained at the same time. The problems of explaining quantitatively these extremely small cross sections are still open.

TABLE V. Total cross sections of reaction (p,n) at 155 MeV (Ref. 10).

Reaction	σ (mb)
^{10}B $(p,n)^{10}$C	0.65 ± 0.1
^{11}B $(p,n)^{11}$C	3.5 ± 0.2
^{13}C $(p,n)^{13}$N	1.9 ± 0.2
^{14}N $(p,n)^{14}$O	0.075 ± 0.01

ACKNOWLEDGMENT

The author would like to express his gratitude to Professor J. Humblet and all the staff for the kind hospitality extended to him at the Institut de Physique, Université de Liège. It should also be acknowledged that this work was done on the financial support of the Institut Interuniversitaire des Sciences Nucléaires, Belgium.

*Researcher, Institut Interuniversitaire des Sciences Nucleaires.

[1]D. T. Chivers, J. J. Domingo, E. M. Rimmer, R. C. Witcomb, B. W. Allardyce, and N. W. Tanner, Phys. Lett. **26B**, 573 (1968).

[2]D. H. Wilkinson, in Proceedings of the International Conference on Nuclear Structure, Tokyo 1967 (unpublished), pp. 469–494.

[3]Y. Sakamoto, Phys. Lett. **29B**, 88 (1969).

[4]K. Bjørnenak, J. Finjord, and P. Osland, Nucl. Phys. **B22**, 179 (1970); F. H. Bakke and A. Beitan, Nucl. Phys. **B20**, 327 (1970).

[5]Il-T. Cheon and A. Tohsaki, Nucl. Phys. **B6**, 585 (1968); D. S. Koltun and A. Reitan, Phys. Rev. **141**, 1413 (1966); S. G. Eckstein, Phys. Rev. **129**, 413 (1963).

[6]G. F. Chew and F. E. Low, Phys. Rev. **101**, 1570 (1956).

[7]J. M. Mckinley, Rev. Mod. Phys. **35**, 788 (1963).

[8]K. M. Watson, Phys. Rev. **89**, 575 (1953).

[9]H. N. Pendleton, Phys. Rev. **131**, 1833 (1963).

[10]L. Valentin, Nucl. Phys. **62**, 81 (1965).